JGR Atmospheres

RESEARCH ARTICLE
10.1029/2021JD035606

# Understanding the Paths of Surface Ozone Abatement in the Los Angeles Basin

**Si-Wan Kim[1,2], Brian C. McDonald[3], Seunghwan Seo[1], Kyoung-Min Kim[1], and Michael Trainer[3]**

[1]Department of Atmospheric Sciences, Yonsei University, Seoul, South Korea, [2]Now at Irreversible Climate Change Research Center, Yonsei University, Seoul, South Korea, [3]NOAA Earth System Research Laboratory, Chemical Sciences Laboratory, Boulder, CO, USA

**Key Points:**

- Long-term trends of ozone and its precursors concentrations in the LA Basin were simulated with the WRF-Chem model
- Weekday and weekend ozone were almost identical or weekday ozone is higher than weekend ozone in the 2010s in the observation and model
- The model indicates that further reduction of $NO_x$ emissions decreases ozone in LA

**Supporting Information:**

Supporting Information may be found in the online version of this article.

**Correspondence to:**

S.-W. Kim,
siwan.kim@yonsei.ac.kr

**Citation:**

Kim, S.-W., McDonald, B. C., Seo, S., Kim, K.-M., & Trainer, M. (2022). Understanding the paths of surface ozone abatement in the Los Angeles Basin. *Journal of Geophysical Research: Atmospheres*, *127*, e2021JD035606. https://doi.org/10.1029/2021JD035606

Received 23 JUL 2021
Accepted 16 JAN 2022

**Author Contributions:**

**Conceptualization:** Si-Wan Kim, Brian C. McDonald, Michael Trainer
**Data curation:** Si-Wan Kim, Brian C. McDonald, Seunghwan Seo, Kyoung-Min Kim
**Formal analysis:** Si-Wan Kim, Brian C. McDonald, Seunghwan Seo, Kyoung-Min Kim, Michael Trainer
**Funding acquisition:** Si-Wan Kim, Michael Trainer
**Investigation:** Si-Wan Kim, Brian C. McDonald, Seunghwan Seo, Michael Trainer
**Methodology:** Si-Wan Kim, Brian C. McDonald, Seunghwan Seo, Kyoung-Min Kim
**Project Administration:** Si-Wan Kim, Michael Trainer
**Resources:** Si-Wan Kim, Michael Trainer



**Abstract** Ozone in the urban atmosphere can accumulate from photochemistry involving nitrogen oxides, carbon monoxide, and volatile organic compounds mainly emitted from fossil fuel combustions and volatile chemical products. Concentrated ozone near the earth's surface has a detrimental impact on the ecosystem and our health. The Los Angeles Basin is a classic example of an urban region with long-standing ozone pollution, frequently in violation of its standard, designated by the US Environmental Protection Agency (EPA). Studies have reported substantial declines of ozone and their precursor concentrations over the past half century in this area due to extensive pollution controls. Since 2000, however, the ozone design value has remained the same and has not been able to fully reach the air quality standard set by the EPA despite decreases in its precursor concentrations. To understand this phenomenon, we utilize a chemical transport modeling approach to reproduce historical ozone trends and to conduct sensitivity runs relative to a 2010 baseline. Based on our analysis of the model simulations comparing the weekends and weekdays, rather than focusing only on the weekly averages, we diagnose that the Los Angeles Basin is actually going under a significant transition in photochemistry toward a lower ozone concentration. This reveals how air quality management strategies are slowly moving towards a pathway of reducing ozone concentrations in the future. Our study, however, suggests that further reductions of $NO_x$ emissions can lead to continued improvement of ozone pollution in this area.

## 1. Introduction

Ozone ($O_3$) in the low atmosphere or troposphere is the most pervasive photochemical oxidant and an important component of smog that poses significant threats to the health of human and ecosystem (National Research Council, 1991). It is currently a major air pollutant that does not meet the environmental standard in the U.S. despite long-term regulations under national air quality programs (e.g., Clean Air Act).

$O_3$ in the troposphere is formed via a photolysis of nitrogen dioxide ($NO_2$) and is then depleted by reacting with nitric oxide (NO) and reproducing $NO_2$. This is a null cycle balancing NO, $NO_2$, and $O_3$ in a photo-stationary state.

$$NO_2 + hv \rightarrow NO + O \quad (1)$$

$$O + O_2 + M \rightarrow O_3 + M \quad (2)$$

$$NO + O_3 \rightarrow NO_2 + O_2 \quad (3)$$

$O_3$ in the urban area can accumulate to a harmful level beyond photo-stationary state via the reactions including carbon monoxide (CO), volatile organic compound (VOC), and nitrogen oxides ($NO_x = NO + NO_2$) in the presence of sunlight. These chemicals are mainly emitted from mobile sources in the urban areas. Historically, CO and VOC (Reactive Hydrocarbon, hereafter RH in the chemical reaction sets below) were emitted mainly from gasoline-fueled motor vehicles (Parrish et al., 2009; Warneke et al., 2012). Recently, VOCs emitted from volatile chemical products are found to be significant contributors for ozone and secondary organic aerosols (Gkatzelis et al., 2021; Qin et al., 2021; McDonald, de Gouw, et al., 2018; Shah et al., 2020). $NO_x$ is released from both gasoline- and diesel-powered motor vehicles in cities with diesel engines being dominating sources if the same amounts of fuels are consumed (McDonald et al., 2012; Yu et al., 2021).

**Software:** Si-Wan Kim, Brian C. McDonald, Seunghwan Seo, Kyoung-Min Kim
**Supervision:** Si-Wan Kim, Michael Trainer
**Validation:** Si-Wan Kim, Brian C. McDonald, Seunghwan Seo, Kyoung-Min Kim
**Visualization:** Si-Wan Kim, Brian C. McDonald, Seunghwan Seo, Kyoung-Min Kim
**Writing – original draft:** Si-Wan Kim, Brian C. McDonald
**Writing – review & editing:** Seunghwan Seo, Kyoung-Min Kim, Michael Trainer

CO and VOC (RH) in the atmosphere reacts with hydroxyl radical (OH) and generate hydroxy and organic peroxy radicals ($HO_2$, $RO_2$, respectively).

$$CO + OH + O_2 \rightarrow HO_2 + CO_2 \quad (4)$$

$$RH + OH + O_2 \rightarrow RO_2 + H_2O \quad (5)$$

The peroxy radicals convert NO to $NO_2$.

$$HO_2 + NO \rightarrow OH + NO_2 \quad (6)$$

$$RO_2 + NO \rightarrow RO + NO_2 \quad (7)$$

$NO_2$ that is produced from reactions Equations 6 and 7 generates $O_3$ from reactions Equation 1 and 2. This increment of $O_3$ is one of the main ingredients of photochemical smog. The reaction cycles above are disrupted when peroxy radials react with peroxy radicals to produce hydrogen peroxide ($H_2O_2$) or organic peroxide (ROOH) under low $NO_x$ conditions or when $NO_2$ reacts with OH to form nitric acid ($HNO_3$) under high $NO_x$ conditions.

$$HO_2 + HO_2 \rightarrow H_2O_2 + O_2 \quad (8)$$

$$RO_2 + HO_2 \rightarrow ROOH + O_2 \quad (9)$$

$$NO_2 + OH + M \rightarrow HNO_3 + M \quad (10)$$

It has been extensively acknowledged that $O_3$ production is not linearly proportional to the availability of its essential precursors, $NO_x$ and VOC (e.g., National Research Council, 1991). Relative abundancy of VOC and $NO_x$ such as VOC/$NO_x$ is a meaningful indicator to determine $O_3$ production efficiency. If VOC is abundant compared to $NO_x$, $O_3$ formation is more sensitive to availability of $NO_x$, so called "$NO_x$-limited regime." In this case, reducing $NO_x$ concentration leads to the reduction of $O_3$ concentration. In contrast, if $NO_x$ is abundant compared to VOC, $O_3$ formation is more sensitive to availability of VOC, so called "VOC-limited regime" or "$NO_x$ saturated regime." In this case, reducing VOC concentrations leads to the reduction of $O_3$ concentration. For "VOC-limited regime," however, reducing $NO_x$ concentrations can cause increases of $O_3$ by suppressing loss of OH in the reaction (Equation 10) and making more OH available for the initiation of chain reactions (Equation 4) and (Equation 5). Therefore, it is essential to perceive and apply this fundamental principle when implementing the $O_3$ abatement policy.

California is notorious for heavy smog because of its large urban population and meteorological and geographic conditions favorable for accumulation of oxidants formed from the intensive photochemistry (Fujita et al., 2003; Haagen-Smit, 1952; Harley et al., 2005; Jacobson, 2005; Jacobson et al., 1996; Kim et al., 2016; Lawson, 1990; Lu et al., 1997; Marr & Harley, 2002; Ryerson et al., 2013). For the last half-century, there have been extensive efforts to reduce emissions and pollution in the Los Angeles Basin (LA Basin hereafter or South Coast Air Basin, SoCAB) that encompasses the urban area of Los Angeles, Orange, Riverside, and San Bernardino counties in Southern California. Recent studies of California air quality reported much cleaner air in 2010 compared to the 1960s and 1970s: ambient CO, $SO_2$ (sulfur dioxide), $NO_x$, VOC, and $O_3$ have been reduced because of air pollution regulations in spite of a large increase in population over the same period (McDonald et al., 2012, 2013; Pollack et al., 2013; Russell et al., 2012; Warneke et al., 2012). In general, the U.S. $O_3$ pollution also improved substantially in response to decreasing $NO_x$ and VOC emissions (Simon et al., 2015). However, as shown in Figure 1, the $O_3$ design values at the 16 sites in the LA Basin have not decreased substantially since 2010 and did not meet the National Ambient Air Quality Standards (NAAQS) for ground-level ozone (70 ppb) designated by the US Environmental Protection Agency (EPA). Here the $O_3$ design value is defined as the 4th highest daily maximum 8 hr-average for three consecutive years. It is important to understand the underlying causes for the $O_3$ trends in this area and prognose the possible future of the trends based on the emission scenario.

$O_3$ in this area can be affected by multiple factors including climate change related phenomena such as heat wave, drought, and wildfires, and changes in background ozone values that are influenced by global or Asian emission changes (Jaffe et al., 2018; Lin et al., 2017). Warmer air may lead to increase $O_3$ production via enhanced chemical reaction rates. Increasing daily mean and maximum temperature trends were observed in the LA Basin (see Figures S1 and S2 in Supporting Information S1). Therefore, the effects of increasing temperature and heatwave events on ozone production will need to be investigated. Meanwhile, drought can reduce $O_3$ concentration by

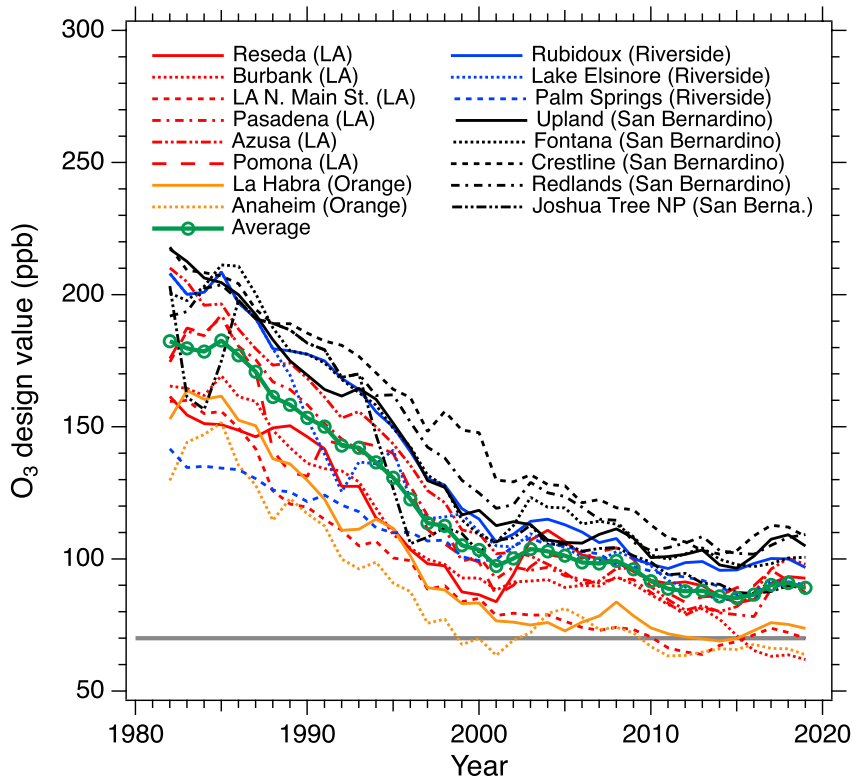


**Figure 1.** $O_3$ design value trends at the 16 monitoring sites in the LA Basin from 1980 to 2019. Here the $O_3$ design value is calculated as the 4th highest daily maximum 8 hr average for three consecutive years. Only the data for May–September (traditional ozone season) are used.

decreasing biogenic emissions (Demetillo et al., 2019) or aggravate $O_3$ pollution by reduced ozone removals over water-stressed vegetation (Lin et al., 2020). A balance between decreased ozone productions and reduced ozone losses would ultimately determine whether $O_3$ concentrations increase or decrease. Palmer Drought Severity Index averaged over the LA Basin indicated drier air in this area since 2000 (see Figure S3 in Supporting Information S1). Thus, the impact of increasing drought events on $O_3$ in the LA Basin will need to be studied. Because of multiple factors affecting $O_3$ concentrations and their complicated interplays, in this study, we rather focus on the responses of $O_3$ in Southern California only to the local anthropogenic emission changes, and aim to provide a precise reasoning on how one factor impacts the $O_3$ level in this area.

Regional chemical transport modeling of long-term trends of air quality can provide detailed information of changing chemistry and transport within the basin and beyond. Early chemical transport modeling studies of the Southern California reasonably reproduced ozone and its precursors for the case (27–29 August 1987) of the Southern California Air Quality Study (SCAQS) and indicated needs for improvement of emissions of CO and VOC (Harley, Russell, McRae, et al., 1993; Harley, Rusell & Cass, 1993). The fuel-use based motor vehicle emission inventory was first applied to the modeling of Southern California for summer 1987 and showed the improved model ozone simulation, compared to the model results utilizing the official inventory (Harley, Sawyer & Milford, 1997). Recent studies also reported that adopting the fuel-use based emission inventory was effective for air quality models to reproduce the chemical observations during intensive field campaigns such as the California Nexus of Air Quality and Climate Change (CalNex) in 2010 (Kim et al., 2016) and the Southeast Nexus (SENEX) in 2013 (McDonald, McKeen, et al., 2018). Furthermore, decadal changes in the motor vehicle emissions and ozone were analyzed and modelled, predicting similar ozone levels in 1997 and 2010 (Harley et al., 2005; Martien & Harley, 2006). In this study, we utilize the Fuel-based Inventory of Vehicle Emissions (FIVE) to simulate long-term air quality in the Los Angeles Basin with a regional chemical transport model. The model reasonably reproduces the change in abundance of ozone and its precursors in the past decades, which enables us to explore the current and future behavior of these species with respect to the pollution policies implemented and provide insights on effective air quality management plans in the near future.

In this manuscript, the methods involving the emission inventory, model experiments, and observational data used in this study are described in Section 2. The results from long-term air quality modeling and evaluation for the past decades and the analyses of model simulations based on future emission scenarios are given in Section 3. Finally, insights for future air pollution-control policies to attain the air quality standard for ozone in the LA Basin are addressed in the conclusions.

## 2. Method

### 2.1. Emission Inventory

In this study, we estimate long-term trends of mobile source emissions and volatile chemical products (VCPs = coatings, inks, adhesives, personal care products, cleaning agents, and pesticides) for the Los Angeles basin, based on methods of McDonald, de Gouw, et al. (2018); McDonald, McKeen, et al. (2018). The text below describes how mobile source and VCP emissions are estimated over time in the Los Angeles basin. All other area and stationary source sectors are taken from merging the California Emissions Almanac 2009 and 2016 (California Air Resources Board, 2009; California Air Resources Board, 2016).

#### 2.1.1. Mobile Sources

We utilize the FIVE as in McDonald et al. (2012, 2013, 2014, 2015); McDonald, de Gouw, et al. (2018); McDonald, McKeen, et al. (2018); and Kim et al. (2016). FIVE reports a fuel-based estimate of $CO_2$, CO, $NO_x$, and VOC emissions from on-road and off-road engines, using taxable fuel sales and roadway or laboratory measured emission factors for gasoline- and diesel-powered vehicles. For on-road transportation, FIVE performs separate spatial and temporal mapping of on-road gasoline and diesel emissions, utilizing highway traffic count, weigh-in-motion, and fuel sales data that distinguish between the two classes of engines. For example, in FIVE, large decreases in diesel engine activity on weekends relative to weekdays are taken into account, as well as separate diurnal profiles for gasoline and diesel engines that vary between weekdays and weekends. Running exhaust emission factors are from roadside infrared remote sensing (Bishop & Stedman, 2008) and tunnel studies (Ban-Weiss et al., 2008), and scaled to account for cold-starting engines (CARB, 2015). For off-road transportation, spatial and temporal mapping are based on surrogates provided by the National Emissions Inventory (NEI) 2005. Emission factors of off-road engines are based on laboratory measurements and summarized previously (McDonald et al., 2015; McDonald, de Gouw, et al., 2018; McDonald, McKeen, et al., 2018). For gasoline-related VOCs, non-tailpipe sources are scaled relative to on-road and off-road gasoline exhaust emissions (McDonald, de Gouw, et al., 2018). We expect non-tailpipe sources of gasoline-related VOCs to decrease at similar rates to tailpipe sources based on long-term ambient VOC measurements in Los Angeles of gasoline tracers (Warneke et al., 2012) and VOC source apportionment analysis (McDonald et al., 2013).

#### 2.1.2. Volatile Chemical Products

We also make estimates of how use of organic solvents (also recently referred to as VCPs) (McDonald, de Gouw, et al., 2018; Qin et al., 2021; Zhu et al., 2019) have trended over time. McDonald, de Gouw, et al. (2018) subdivided VCPs into six categories: coatings, inks, adhesives, personal care products, cleaning agents, and pesticides. Here, we utilize the Economic Census Survey (U.S. Census Bureau, 1995) and Commodity Flow Survey (U. S. Bureau of Transportation Statistics, 1996) reported for the year 1992 to estimate the amount of organic solvent mass consumed by these six VCP sectors (Table S1 in Supporting Information S1). For reference, we also include the organic solvent mass reported by McDonald, de Gouw, et al. (2018) utilizing the Economic Census Survey and Commodity Flow Survey in 2012. Briefly, we follow the methodology of McDonald, de Gouw, et al. (2018). The Economic Census Survey is reported by the US Census Bureau every 5 years and provides economic information on the dollar amount of chemical products sold and materials consumed, including information on the types of chemicals utilized in manufacturing (Table S1, column 2 in Supporting Information S1). To convert from dollar to mass units, we utilize the Commodity Flow Survey, which is reported by the US Department of Transportation every 5 years, and which provides economic value and mass of chemicals transported. This provides a price conversion factor (Table S1, column 3 in Supporting Information S1) by which we can estimate the mass of organic solvents consumed in volatile chemical products (Table S1, column 4 in Supporting Information S1).

The amount of organic solvent mass emitted to the atmosphere depends on the volatilization fraction (amount of VOC emitted per amount of organic solvent dispensed). The volatilization fraction depends on the chemical product type, and is highest for coating-related products (~90%) that continuously emit to the atmosphere after applied, and

lowest for cleaning products (~15%), which can be disposed down-the-drain. The volatilization fraction is taken from McDonald, de Gouw, et al. (2018), and assumed to be relatively constant over time, since the volatilization fraction is more strongly a function of how a chemical product is used than its formulation. Thus, we take the trend in organic solvent mass (Table S1 in Supporting Information S1) as a proxy for VCP emission trends (Table S2 in Supporting Information S1) by sector. McDonald, de Gouw, et al. (2018) report VOC emissions by chemical product type for SoCAB in 2010. We extrapolate the 20-year trends in Table S1 in Supporting Information S1 (1992–2012) over a 23-year time frame (1987–2010) to scale 2010 VOC emissions from VCPs to 1987. McDonald, de Gouw, et al. (2018) report emission uncertainties that take into account the quantification of the organic solvent mass using economic surveys and volatilization fraction by chemical product type. Individual VCP sectors exhibit emission uncertainties ranging from 25% to 75% (see Table S2 in Supporting Information S1).

Over a twenty-year period, we estimate roughly a factor of 2 decrease in the organic solvent mass consumed by VCPs, reflecting efforts to reduce the VOC content of everyday chemical products, including for their potential to form ground-level ozone (EPA, 1995). An example is the coatings sector, and the shift from solvent-borne to lower VOC water-borne formulations (Stockwell et al., 2021). Between 1987 and 2010, we estimate the largest reductions in VCP emissions for printing inks (−60%), followed by adhesives (−57%), coatings (−42%), personal care products (−40%), pesticides (−25%), and cleaning agents (−24%). Recently, Coggon et al. (2021) reports ozone production efficiency for individual VCP categories for a high ozone event in New York City exhibiting VOC sensitivity. The ozone formation potential is within 30% for coatings, adhesives, personal care products, and cleaning agents, which are the four largest VCP emission sectors. The ozone formation potential of pesticides and printing inks are noticeably higher, though they do not contribute greatly to the total. In this study, we extrapolate VCP emissions across the different modeling years of the study based on Table S2 in Supporting Information S1 for SoCAB. Table S2 in Supporting Information S1 summarizes the bottom-up VOC emissions used in this study for VCPs in 1987 and 2010, and shows the absolute magnitude in relation to mobile sources and petrochemical facilities.

#### 2.1.3. FIVE-VCP Emission Trends

Kim et al. (2016) successfully simulated the day of week variations of CO, $NO_x$, and $O_3$ using FIVE in the LA Basin during the period of CalNex field campaign in 2010, with a focus on mobile source emissions. In this study, we combine the FIVE mobile source and VCP inventory (herein referred to as FIVE-VCP, Coggan et al., 2021) for $NO_x$, CO, and VOC encompassing from 1987 to 2010 to simulate long-term air quality trends in the LA Basin. Figure 2 shows the trend of the FIVE-VCP $NO_x$, CO, and VOC emissions in the Basin from 1985 to 2014. The normalized trends of the emissions relative to the values in 1987 are also shown in Figure 2, which is the first year of our model simulations. The model runs are conducted for five years (1987, 1997, 2002, 2005, and 2010) that capture the main changes in the trends (symbols in Figures 1 and 2; emission values in Table 1). The FIVE-VCP inventory shows significant declining trends of $NO_x$, CO, and VOC emissions in this area for these three decades. Continued efforts to decrease emissions from on-road gasoline and diesel-powered engines as well as stationary sources reduced $NO_x$ emissions in the LA Basin more than 50% compared to the value in 1987 over a 25 year period (Figure 2). Historically, on-road gasoline engines were the most important source for CO emissions. Therefore, regulating this type of on-road mobile source led to almost 80% reduction of total CO emissions in this area from 1987 to 2010 (Figure 2). In 2010 and later, the CO emissions from off-road gasoline engines are as important as those from on-road gasoline engines in this region. Similar to CO, VOC has gone down substantially by regulating emissions from on-road gasoline engine sources. In the inventory, VCPs remain an important source of VOC emissions, and which have not decreased as much (by factor of ~2) compared to those from mobile sources (by factor of 4–5) between 1987 and 2010 (Table S2 in Supporting Information S1). The reduction of total VOC emissions is about 60%–70% compared to the value in 1987 (Figure 2). Currently, it has been suggested that VCPs are the largest source of anthropogenic VOC in the Los Angeles basin and recent modeling studies have shown significant effects on ozone and aerosol concentrations (Qin et al., 2021; McDonald, de Gouw, et al., 2018; Zhu et al., 2019).

### 2.2. Regional Chemical Transport Model and Experiments

We use the version 3.4.1 of the Weather Research and Forecasting-Chemistry model (WRF-Chem, Grell et al., 2005), which has been tested extensively against meteorological and chemical observations acquired from several field campaigns in the US (Ahmadov et al., 2015; Kim et al., 2011; Kim et al., 2016; McDonald, McKeen,

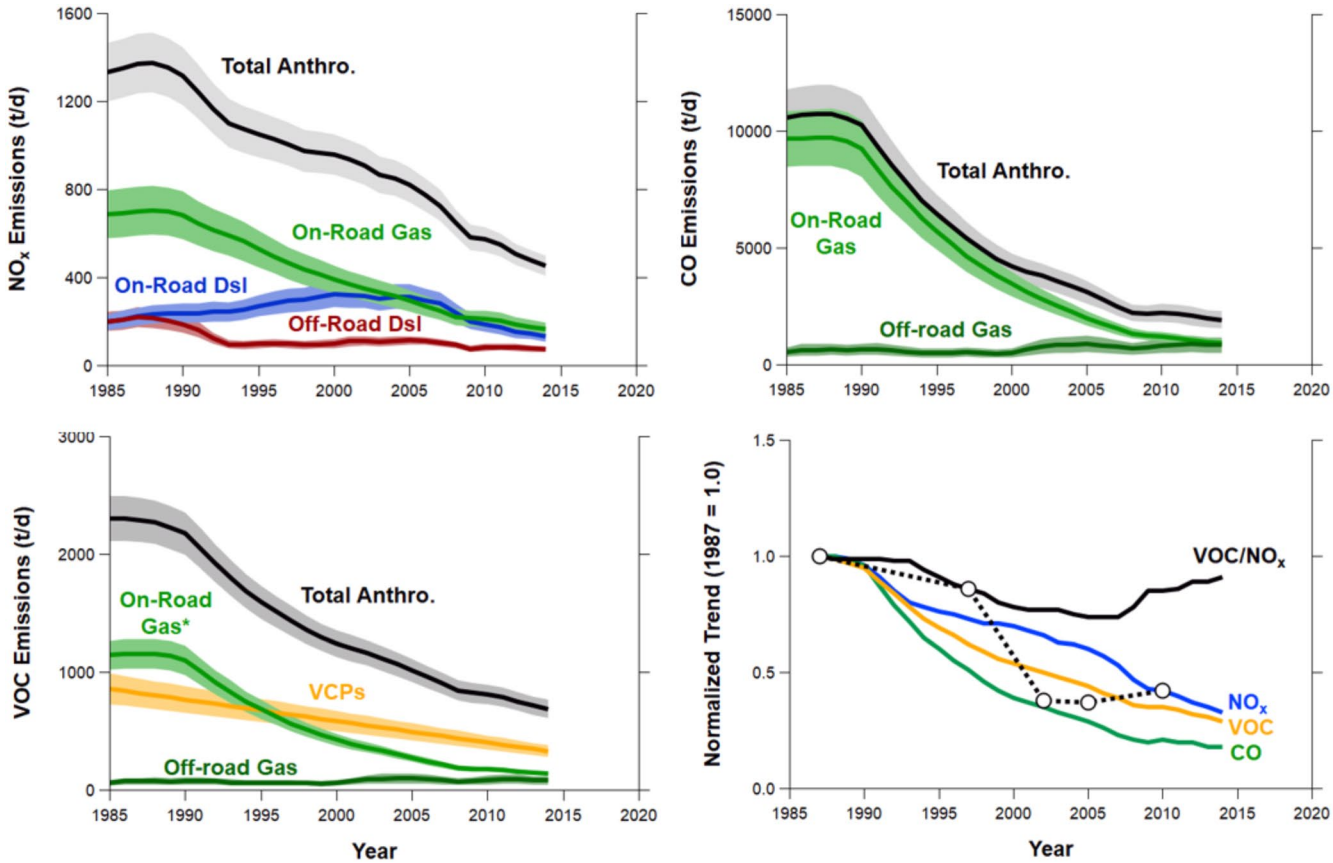


**Figure 2.** Trends of the FIVE-VCP (top left) $NO_x$, (top right) CO, and (bottom left) volatile organic compound (VOC) total and sectoral emissions (ton $day^{-1}$, t/d) in the Los Angeles Basin (or South Coast Air Basin) from 1987 to 2014. Solid lines show the emissions trends in the bottom-up inventory and bands show the uncertainty in activity and emission factors for all anthropogenic emissions (black lines) and key emission sectors. Non-tailpipe gasoline emissions of VOCs are included with on-road gasoline sources and denoted by the asterisk. Trends of the FIVE-VCP emissions normalized to the values in 1987 for $NO_x$, VOC, CO and VOC/$NO_x$ (solid lines) (bottom right). The top-down model adjusted VOC/$NO_x$ emissions trend is shown by the dashed black line and open markers denote model years simulated in WRF-Chem.

et al., 2018). The domain of the WRF-Chem model is the western U.S. (12 × 12 km horizontal resolution) that mainly covers the state of California. The model has 60 vertical levels with ~50 m thickness between vertical levels up to 4 km from the ground level, with coarser vertical resolutions at higher levels. The first model level where mixing ratios of chemical species are calculated is ~25 m. The simulation period is a typical ozone season from 1 May to 30 September for the 5 years of 1987, 1997, 2002, 2005, and 2010 that captures the main features of long-term trends of ozone and its precursor. Meteorological initial and boundary conditions are based on the ECMWF Era-Interim data (Berrisford et al., 2011). The model adopts a specific meteorological condition pertaining to each year. However, it would be best to continuously simulate all years from 1987 to 2010 and beyond, to thoroughly investigate inter-annual variations of $O_3$ in association with weather and large-scale climate variability. Biogenic emissions are based on the Model of Emissions of Gases and Aerosols from Nature (MEGAN) (Guenther et al., 2006). The Noah land surface model, Yonsei University planetary boundary layer model, and Lin microphysics scheme are adopted (see references in Kim et al., 2009). The chemical mechanism is based on the Regional Atmospheric Chemistry Mechanism (RACM) (Stockwell et al., 1997) with ~30 reaction rate coefficients updated (Kim et al., 2009) and has been widely tested (Ahmadov et al., 2015; Kim et al., 2011; Kim et al., 2016; McDonald, McKeen, et al., 2018).

**Table 1**
*FIVE Emission Estimates for California's South Coast Air Basin (Metric Tons/day) Used in This Study*

| | Species | | |
|---|---|---|---|
| Year | $NO_x$ | CO | VOC |
| 1987 | 1 370 | 22 000[a] | 4 600[a] |
| 1997 | 1 000 | 10 900[a] | 2 900[a] |
| 2002 | 910 | 3 800 | 1160 |
| 2005 | 820 | 3 100 | 1020 |
| 2010 | 570 | 2 200 | 810 |

*Note*. The CO and VOC emissions in 1987 and 1997 are modified from FIVE.
[a]The FIVE-VCP emissions were approximately doubled.

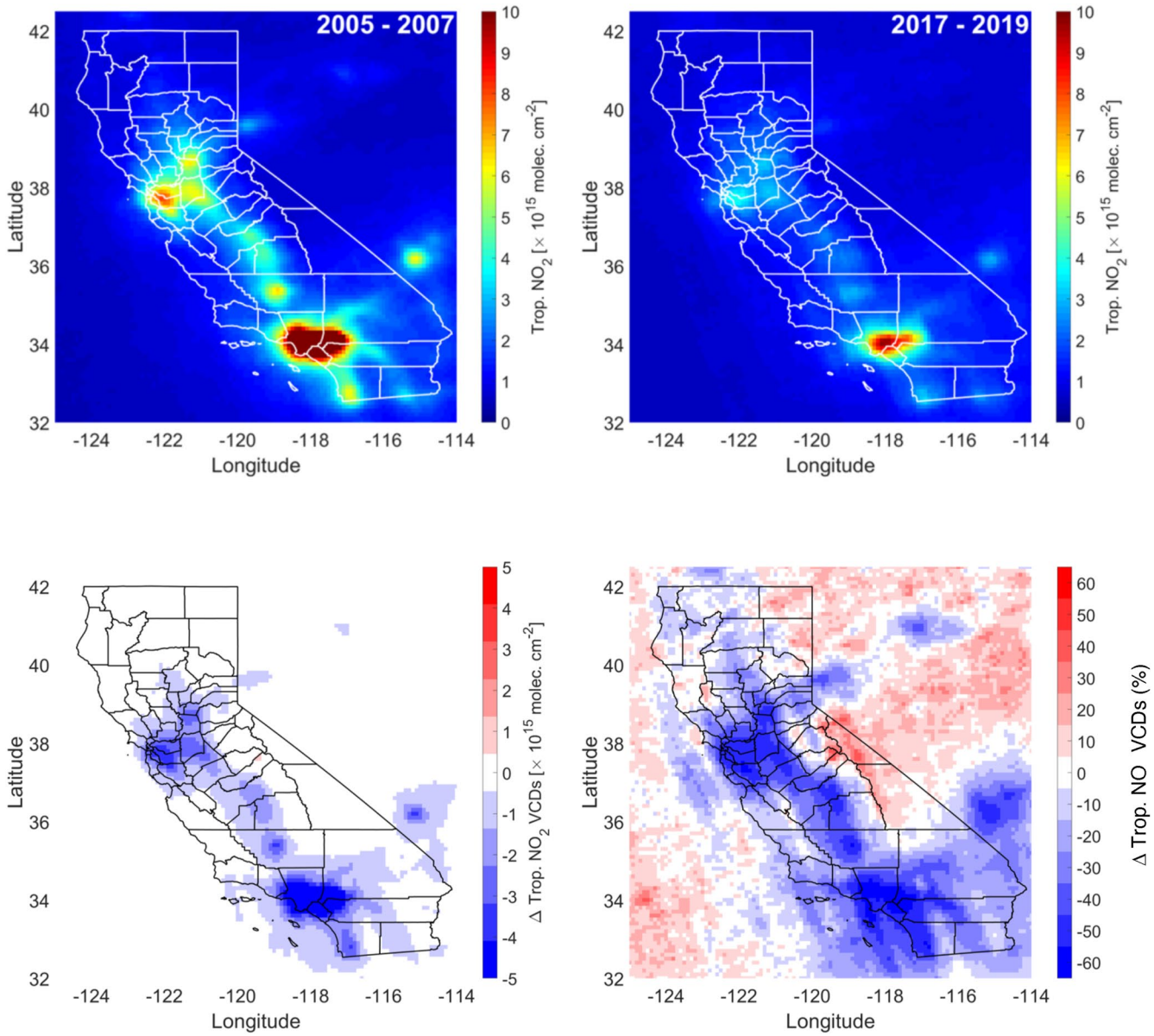


**Figure 3.** Ozone Monitoring Instrument tropospheric $NO_2$ vertical column density (VCD) in California averaged for 2005–2007 (top left) and 2017–2019 (top right), absolute differences between the two period (bottom left), and fractional differences (%) (bottom right).

To focus on the impact of local anthropogenic emission changes, we did not adopt the chemical boundary conditions from global models that incorporated Asian emission changes. Thus, the chemical boundary condition does not vary inter-annually. Wildfire emissions were not included in the simulations for the same reason.

### 2.3. Long-Term Observational Data Sets

#### 2.3.1. AQMD Surface Monitoring Data

The hourly $NO_x$, CO, and $O_3$ data from the South Coast Air Quality Management District (AQMD) monitoring network (http://www.arb.ca.gov/aqmis2/aqdselect.php) are utilized to evaluate the model simulations. AQMD uses chemiluminescence detection with a Molybdenum converter to measure surface $NO_2$. Other oxygenated nitrogen species are known to contribute to the $NO_2$ measured by this method (Dunlea et al., 2007; Fehsenfeld et al., 1987). Although the AQMD measurements may not be as accurate as the field measurements obtained during the inten-

sive field campaigns such as CalNex (Ryerson et al., 2013), these routine monitor data are available for many decades and can serve as a main evaluation data set for air quality modeling research that examines long-term trends. To minimize the interference from oxygenated nitrogen species other than $NO_2$, we utilized the observations in the morning when the emissions from mobile sources are large and the formation of oxygenates via photochemistry is negligible. For $O_3$, we used the data from May to September, calculated daily maximum 8 hr-average values, and presented the 95th, 90th, 75th, 50th, and 25th percentiles of those values as well as the averages.

### 2.3.2. Satellite Remote Sensing Data

To understand the recent changes in the $NO_x$ emissions, the trends of satellite Ozone Monitoring Instrument (OMI) tropospheric $NO_2$ column data were analyzed (Figure 3). The OMI is on board the EOS-Aura satellite and was launched into a sun-synchronous orbit in 2004, with a low-Earth orbit, overpassing at approximately 13:45 local time (Boersma et al., 2011; Levelt et al., 2006; Levelt et al., 2018). We utilized Version 4.0 daily OMI level 3 tropospheric column $NO_2$ data available from the NASA Aura validation data center with a spatial resolution of $0.1° \times 0.1°$. The plot is generated by including high quality clear-sky data with effective cloud fraction <0.3. Information on the $NO_2$ retrieval algorithm can be found in Lamsal et al. (2021). In Figure 3, the OMI data indicate substantial decreases of tropospheric $NO_2$ columns in California between 2005 and 2019 (May–September).

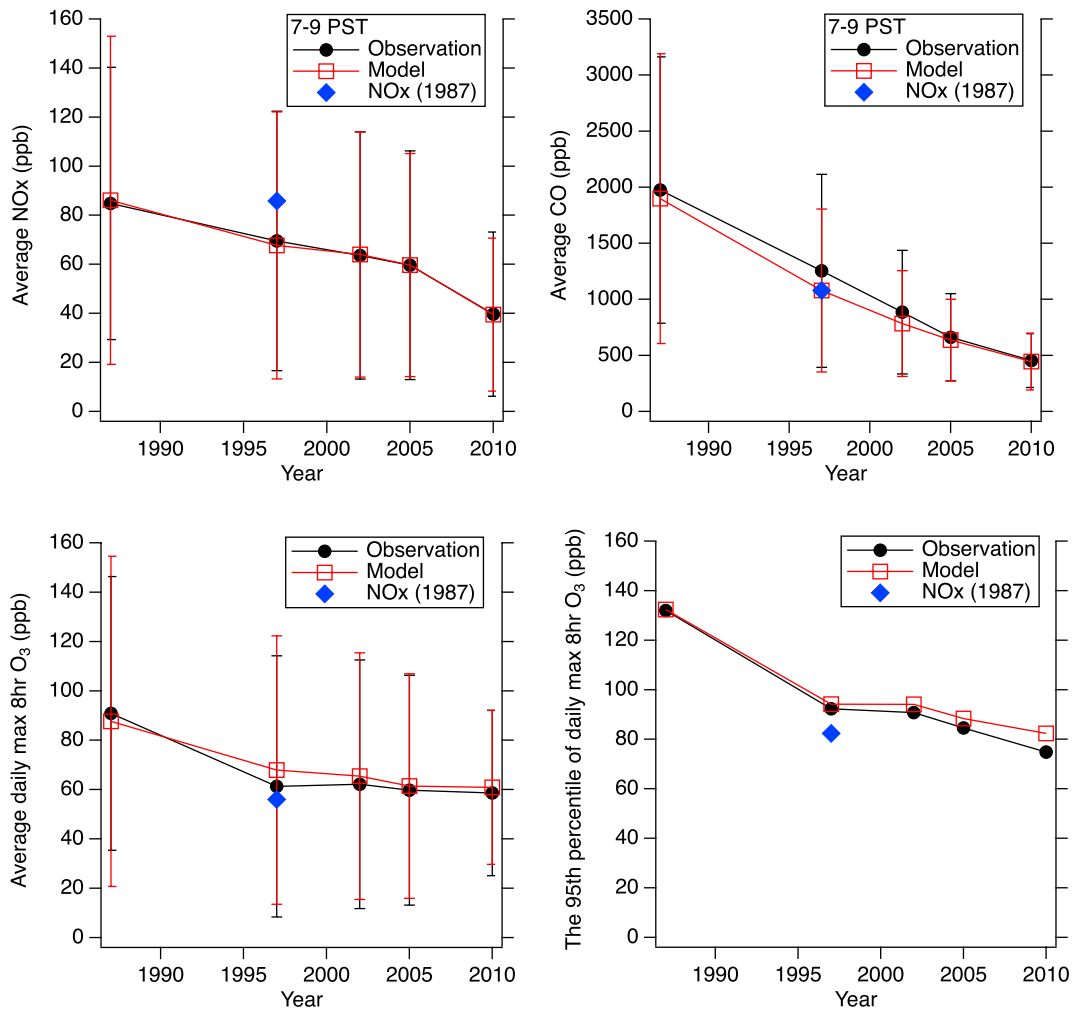


**Figure 4.** Evaluation of the model simulations with the surface observations of (top left) $NO_x$ at 7–9 PST, (top right) CO at 7–9 PST, (bottom left) averages of daily maximum 8 hr average $O_3$, and (bottom right) the 95th percentile of daily maximum 8 hr average $O_3$ from May to September in 1987, 1997, 2002, 2005, and 2010. Blue diamond symbol represents the model results for 1997 that replaced the $NO_x$ emissions to 1987 level. Black (red) solid line with filled circles (open squares) denotes observations (model). The vertical bars represent standard deviation. The observations at the 16 sites displayed in Figure 1 and the model results sampled at the corresponding sites are compared.

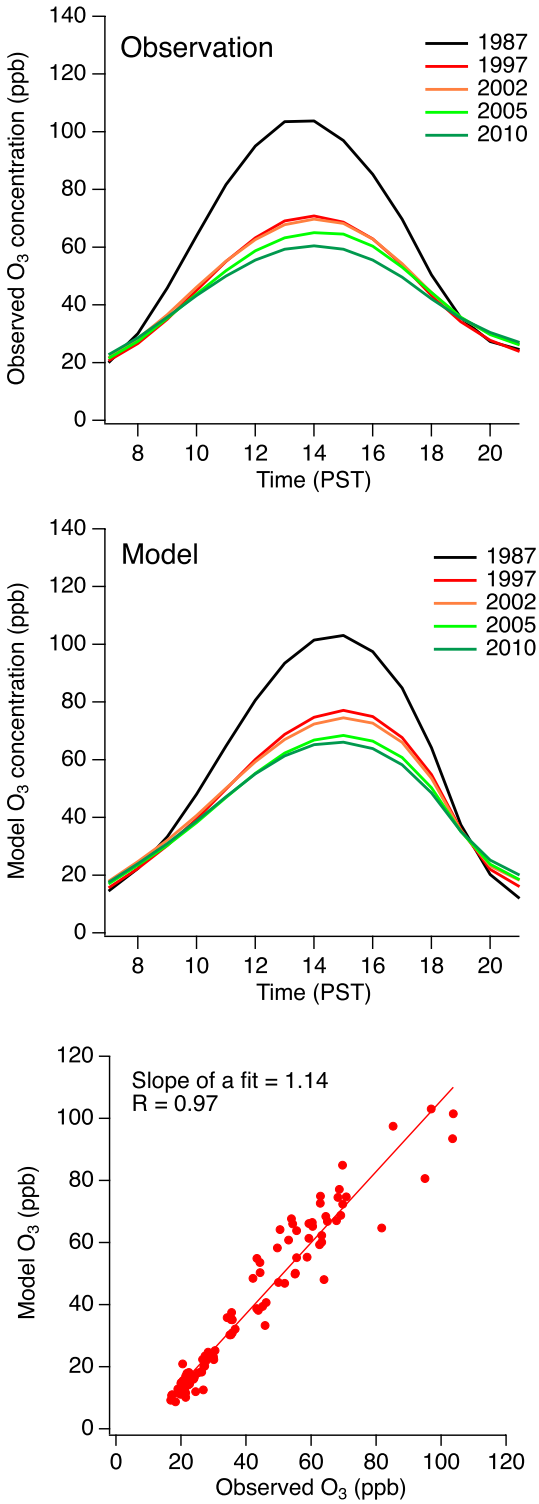


**Figure 5.** Comparison of diurnal variations of the observed and simulated $O_3$ in the LA Basin from May to September in 1987, 1997, 2002, 2005, and 2010. The observations at the 16 sites displayed in Figure 1 and the model results sampled at the corresponding sites are compared.

In the LA Basin, the OMI $NO_2$ columns were reduced by approximately 60% between 2005 and 2019. Thus, it is clear that $NO_x$ emissions significantly decreased while $O_3$ concentrations were steady in the recent years (Figure 1).

## 3. Results

### 3.1. Evaluation of the Model Results With the Surface Observations (1987–2010)

First, we evaluated the model results with the observations from the surface monitoring sites in the LA Basin. The CO, $NO_x$, and $O_3$ concentrations averaged for the typical ozone season from 1987 to 2010 are shown (Figure 4). Both the observed and simulated CO concentrations reduced from 1975 ppb in 1987 to 454 ppb in 2010 by 77%. Both the observed and simulated $NO_x$ concentrations declined from 85 ppb in 1987 to 40 ppb in 2010 by 53%. The averages of daily maximum 8 hr-average $O_3$ concentrations measured at the surface monitoring sites decreased substantially from 1987 to 2000 by 32%, but it showed only small changes after 2000, in spite of substantial decreases of the precursor concentrations as shown in Figures 2 and 4. The model $O_3$ changes mainly driven by the anthropogenic emission changes in this study showed similar features to the observations. The 95th percentile of daily maximum 8 hr-average $O_3$ in the ozone season (May–September) from the measurements and model simulations exhibits similar trends, although the model continues to decrease even after 2000 (to 2010). In general, the model using FIVE-VCP successfully reproduced the long-term changes in the observed $NO_x$ concentrations. However, the model using FIVE-VCP underestimated the CO and $O_3$ concentrations in the earlier years, such as 1987 and 1997. Through several emission sensitivity tests, we found that doubling the CO and VOC emissions in FIVE-VCP only for 1987 and 1997 enabled the model to more accurately simulate the ambient CO and $O_3$ concentrations in Figure 4. This leads to a factor of ~2 sharper drop in the VOC/$NO_x$ emissions ratio in the model-adjusted simulations than in the bottom-up inventory between 1987 and 2010 (Figure 2). The emission estimations used for the modeling are summarized in Table 1.

In the past (e.g., 1987), both CO and VOC are expected to be mainly from on-road gasoline sources, including tailpipe and non-tailpipe emissions for VOCs (Harley et al., 1992; Warneke et al., 2012; McDonald et al., 2013). The underestimate in FIVE mobile source CO is consistent with Hassler et al. (2016), suggesting that FIVE CO and co-emitted VOCs may be underestimated by ~40%, especially in earlier years for the 1980s and 1990s when on-road emissions dominate both of these species. However, we also note that Harley, Sawyer and Milford (1997) modeled the SCAQS 1987 study period, and was able to simulate observed high ozone using SoCAB $NO_x$ emissions of 1 200 t/d, CO emissions of 8 900 t/d, and anthropogenic VOC emissions of 2 800 t/d. Compared to Table 1, our bottom-up FIVE-VCP emissions of $NO_x$, CO, and VOC are within ~20% of Harley, Sawyer and Milford (1997), while top-down model-adjusted CO and VOC emissions are ~2 times higher. Further investigation is needed on why there are discrepancies between the top-down (model adjusted) and bottom-up (FIVE-VCP) trends of VOC/$NO_x$ emissions in the Los Angeles basin.

A model sensitivity run is conducted to highlight the roles of VOC versus $NO_x$ emission controls on $O_3$ reductions from 1987 to 1997. In this run, the $NO_x$ emissions in 1997 were replaced by a much higher value in 1987 (see Figure 4, blue diamond), which caused lower averaged and the 95th percen-

**Table 2**
*The $NO_x$ Emission Scenarios*

| Case | Emissions: $NO_x$ emissions (metric tons/day) | Note |
|---|---|---|
| LOW $NO_x$ (representing year 2020) | 287 | 50%/10 years reduction from the level in 2010 (Diesel Trucks SCR + Further pollution controls) |
| VERY LOW $NO_x$ (representing year 2030) | 143 | 50%/10 years reduction from the level in 2020 (or the LOW $NO_x$ case)(Mitigation to electric vehicles + Further pollution controls) |

tile $O_3$ concentrations in 1997 compared to the original case: Higher $NO_x$ led to lower $O_3$. Therefore, we conclude that the substantial $O_3$ concentration declines from 1987 to 1997 was mainly due to the VOC emission controls. It also confirms that $O_3$ was in "VOC-limited" regime in this period because of an inverse correlation of $O_3$ and $NO_x$ concentration. This is consistent with Martien and Harley (2006), which found similar decreases in ozone over SoCAB due to faster control of anthropogenic VOCs relative to $NO_x$.

Diurnal variations of modeled $O_3$ concentrations are also evaluated with the observations in Figure 5. The averages of the observations and model results at the 16 monitoring sites (defined in Figure 1) for May–September show similar diurnal profiles and evolutions from 1987 to 2010. The linear fit of the hourly model results to the hourly observations gives the slope of 1.14 and correlation coefficient of 0.97. The modeled peaks occurred an hour later than the observations on average. Both the observations and model results demonstrate the decrease of the average $O_3$ concentrations during daytime from 1987 to 2010. It also shows the increases of the average $O_3$ concentrations during nighttime for the same period due to reduced $NO_x$ emissions (via decreased loss of $O_3$ reacting with NO).

### 3.2. The Model Results From the $NO_x$ Emission Scenario Runs

The model sensitivity runs based on the $NO_x$ emission scenarios in Table 2 were conducted to highlight the roles of $NO_x$ emission controls on $O_3$ reductions from 2010 and onward. In the LOW $NO_x$ case (representing 2020), the $NO_x$ emissions in 2010 were reduced by 50%. The 50% reduction of $NO_x$ emissions from the level in 2010

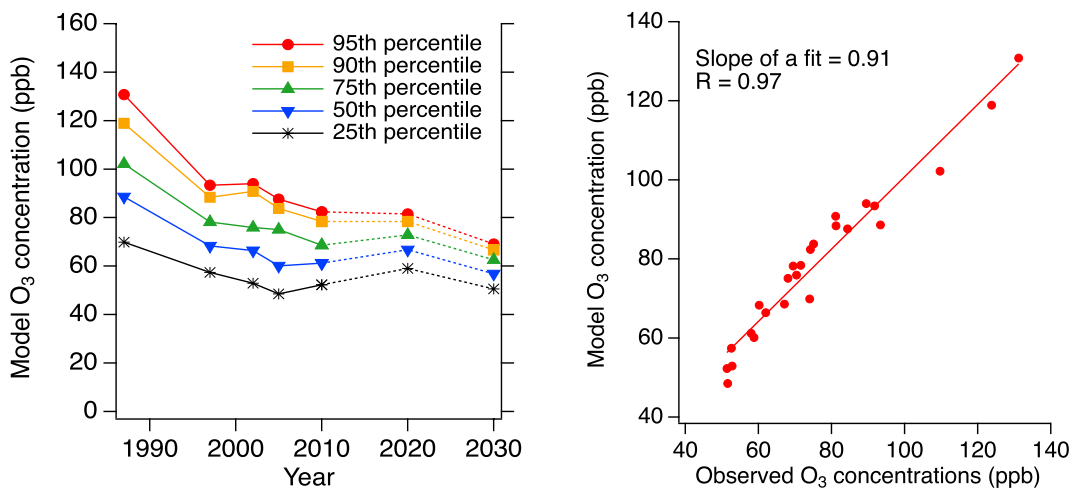


**Figure 6.** The changes in the 95th, 90th, 75th, 50th, and 25th percentiles of daily maximum 8 hr average $O_3$ in the model simulations with time in the LA Basin (left) and evalution of the model values with the corresponding observations (right) from May to September in 1987, 1997, 2002, 2005, and 2010. The data for 2020 and 2030 are the model results based on the $NO_x$ emission scenario cases (see Table 2, the LOW $NO_x$ Case for 2020 and the VERY LOW $NO_x$ case for 2030). The observations at the 16 sites displayed in Figure 1 and the model results sampled at the corresponding sites are utilized. Dashed lines denote the model results based on the $NO_x$ scenario.

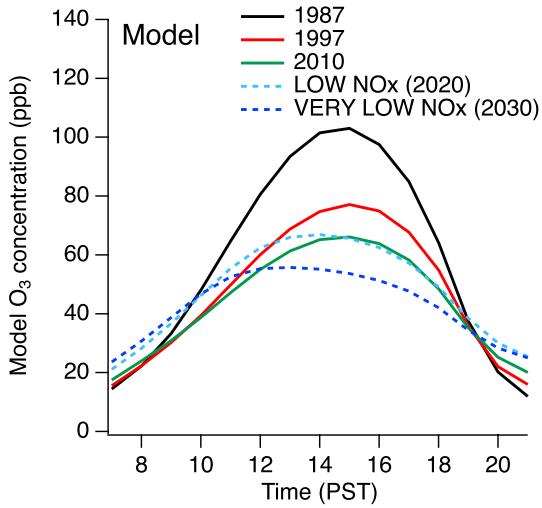


**Figure 7.** Evolutions of diurnal variations of the model $O_3$ in the LA Basin from May to September in 1987, 1997, 2002, 2005, and 2010 (solid lines) and the model $O_3$ concentrations based on the $NO_x$ emission scenarios (dashed lines). LOW $NO_x$ (VERY LOW $NO_x$) denotes 50% (75%) reductions from the value in 2010.

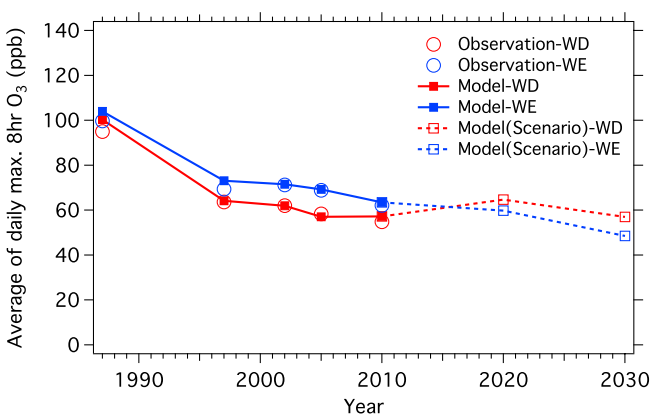


**Figure 8.** Trends of the model-simulated ozone in the LA Basin during weekdays and weekends from May to September in the selected years (1987, 1997, 2002, 2005, and 2010) (solid lines with filled square symbols). The model runs with the $NO_x$ emission scenario that assume 50% and 75% $NO_x$ emissions reduction relative to the value in 2010 are shown as dashed lines with open square symbols. The scenario assumes 50% $NO_x$ emission reductions by 2020 (the LOW $NO_x$ case) and 75% by 2030 (the VERY LOW NOx case) relative to 2010. The scenario runs are based on the same meteorology as in 2010. The averages of daily maximum 8hr-average $O_3$ for the 16 sites in Figure 1 are plotted. The corresponding observed values in 1987, 1997, 2002, 2005, and 2010 are also shown as open circles.

reflects the plan in which heavy-duty diesel-powered trucks in the LA Basin implement Selective Catalytic Reduction (SCR) system by 2020. In reality, heavy-duty truck $NO_x$ has been shown to be higher than expected following widespread deployment of SCR systems (Dixit et al., 2017; Tan et al., 2019). In the VERY LOW $NO_x$ case (representing 2030), 75% reduction of $NO_x$ emissions from the level in 2010 (or 50% reduction from 2020) represents the case in which further decrease of the emission is achieved by partly replacing traditional fossil-fuel based motor vehicles by clean fuel vehicles. In Figure 6, the trends of the 25th, 50th, 75th, 90th, and 95th percentile of daily maximum 8 hr-average $O_3$ concentration from the model simulations are shown. The $O_3$ concentration in the model and observations from 1987 to 2010 reasonably agree with each other (the slope of a linear fit of 0.91 and correlation coefficient of 0.97), presenting declining trends in most of times. However, in the LOW $NO_x$ case (2020 in Figure 6), the 25th to 75th percentile of $O_3$ concentration slightly increases from 2010 while the 90th and 95th percentile stay almost the same in 2010. In contrast, in the VERY LOW $NO_x$ case (2030 in Figure 6), the $O_3$ concentration from the 25th to 95th percentile decreases from the LOW $NO_x$ case (2020 in Figure 6), suggesting that this $NO_x$ emission reduction finally turns the chemical regime from "VOC-limited" to "$NO_x$-limited."

Figure 7 shows the diurnal variation of the model $O_3$ concentration including the sensitivity runs based on the $NO_x$ emission scenarios. In the LOW $NO_x$ case, the $O_3$ concentration at the peak time does not decrease from 2010 while in the VERY LOW $NO_x$ case, the concentration at the peak time decreases compared with the LOW $NO_x$ case and the model results for 2010. Our model results show that the peak times of $O_3$ concentration change to the earlier times in the LOW $NO_x$ and VERY LOW $NO_x$ case compared to 1987–2010. Note that the changes in the $O_3$ peak times occur without changing diurnal profiles of emissions. Much reduced $NO_x$ conditions lead to more enhanced $O_3$ formation in the morning in the scenario runs. The observed changes in $O_3$ peaks times from the beginning of 2010s to the end of 2010s were also investigated (see and Figure S4 in Supporting Information S1). Comparing the ozone concentrations in 2018 or 2019 to those in 2010 indicates that the maximum in recent years slightly shifted to an earlier time. We also compared the averages from 2009 to 2011 with those from 2017 to 2019 and found a similar change. However, it is too early to demonstrate a clear shift. Therefore, this feature will need to be monitored consistently as $NO_x$ emissions decreases further in the future. There are clear increases of the $O_3$ concentration during nighttime in the LOW and VERY LOW $NO_x$ case in Figure 7. The observed nighttime $O_3$ concentrations from 2010 to 2019 show an increasing trend of 0.37 ppb $yr^{-1}$ on average (see Figure S5 in Supporting Information S1). Lower $NO_x$ causes lower $O_3$ loss ($O_3$ + NO) during the nighttime, leading to higher $O_3$ concentrations. Yan et al. (2018) also reported positive nighttime $O_3$ trends in the U.S. due to reduced ozone titration. This model results can be confirmed with the observations in 2020 and onward if there are substantial $NO_x$ emission decreases for the period as in our scenarios. The scenario model runs suggest that improving $NO_x$ control technology for gasoline and diesel engine vehicles, as well as greenhouse gas mitigation could reduce future $O_3$ pollution.

### 3.3. Weekday Versus Weekends: Evolutions

In the LA Basin, $NO_x$ emissions on weekends were substantially decreased by ~50% compared to that on weekdays because of reduced heavy-duty truck activities (Harley et al., 2005; Kim et al., 2016; McDonald et al., 2012). Faster photochemistry on weekends than on weekdays, exhibiting higher $O_3$, $O_x$ (= $O_3$ + $NO_2$), Peroxyacetyl Nitrate (PAN), and HCHO concentration on

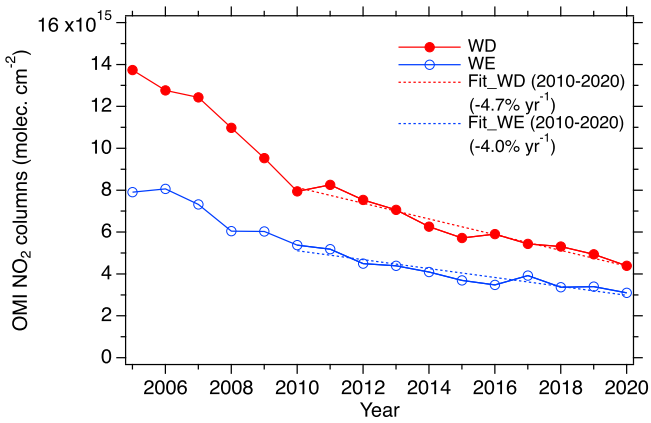


**Figure 9.** Trends of Ozone Monitoring Instrument tropospheric $NO_2$ vertical column density in the LA Basin during weekdays and weekends . The rate of change for weekdays (Fit_WD) is −4.7% $yr^{-1}$ and that for weekends (Fit_WE) is −4.0% $yr^{-1}$.

weekends under the urban "$NO_X$-saturated" or "VOC-limited" chemical regime, was reported based on airborne and ground-based observations (Pollack et al., 2012; Warneke et al., 2013). This feature was also successfully simulated using regional chemical transport models (e.g., Chen et al., 2013; Kim et al., 2016). While higher surface $O_3$ concentrations on weekends remain widespread, an analysis showed that the spatial extent and the trend in the probability of weekend $O_3$ effect occurrences had decreased significantly compared to a decade ago (Baidar et al., 2015). Because of persistent changes in $O_3$ concentration within the week, it would be informative to examine the trend of $O_3$ concentrations for weekdays and weekends separately and to effectively trace the changes in chemical regimes. Figure 8 shows that both observed and simulated $O_3$ concentrations on weekends were persistently higher than that on weekdays from 1987 to 2010, due to non-linear chemistry under a "VOC-limited" regime. The $O_3$ concentrations shown are the average of daily maximum 8 hr-average values. The $O_3$ concentrations on weekends and weekdays were declining from 1987 to 2010, but with a slower rate in 2000s compared to the earlier time. The model results from the LOW $NO_x$ case and VERY LOW $NO_x$ case are shown in the time axis of 2020 and 2030, respectively, in Figure 8. As mentioned, the scenarios (Table 2) are based on the assumption of 50% reduction of $NO_x$ emissions from 2010 to 2020 (LOW $NO_x$ case). Actual changes in $NO_2$ concentrations between 2010 and 2020 that are detected from OMI tropospheric $NO_2$ column observations are demonstrated for weekdays and weekends separately in Figure 9: OMI $NO_2$ columns decreased by approximately 4.7% $yr^{-1}$ for weekdays and by 4.0% $yr^{-1}$ for weekends for the decade. In 2020, the COVID-19 pandemic affected the global $NO_2$ abundances (Bauwens et al., 2020). Reduced vehicles activities in California decreased $NO_x$ emissions by ∼20% in April 2020, compared to the Business-As-Usual case (Harkins et al., 2021). The changes in Figure 9 agrees with those between 2010 and the LOW $NO_X$ case in our scenario. Therefore, we can interpret the $O_3$ simulations from the LOW $NO_x$ case as a proxy for 2020. In Figure 8, the model $O_3$ concentration increases (decreases) on weekdays (weekends) from 2010 to 2020 and the weekdays and weekends $O_3$ concentration get almost identical around the mid of 2010s for the first time in more than 20 years. The slight decrease of the model $O_3$ concentration on weekends from 2010 to 2020 highlights a possible regime change from "VOC-limited" to "$NO_x$-limited." During this period, the $O_3$ concentrations on weekdays are getting higher than those on weekends. With the further $NO_x$ emission reduction as in the VERY LOW $NO_x$ case (or 2030), the $O_3$ concentrations will decline further on both weekdays and weekends between 2020 and 2030 with no weekend $O_3$ effects (Figure 8). The scenarios lead to "$NO_X$-limited" regime from "VOC-limited" regime toward the end of the 2010s.

Finally, to evaluate our model scenario in Figure 8, we analyzed the observed weekday and weekend $O_3$ concentration at the surface monitors, LA North Main Street, Pasadena, Azusa, Upland, Fontana, and Redlands from early 1980s to 2019. In Figure 10, the $O_3$ concentrations on weekdays and weekends are almost identical in the mid to late 2010s at these locations. The concentration here is the average of daily maximum 8 hr-average value. The observed trends at majority of sites agree with the model simulations based on the scenario: increases on weekdays and decreases on weekends from 2010 to the mid to late 2010s and decreasing trends on both weekdays and weekends for several sites toward 2020 (LA N. Main St., Azusa, Upland in Figure 10). The $O_3$ concentration averaged over the 16 sites (as in Figure 1) in the LA Basin also exhibits similar results: $O_3$ concentration decreases on weekends, slightly increases on weekdays from 2010 to 2016 and the values on weekdays and weekends are getting identical in the mid of the 2010s. After 2017, the observed $O_3$ concentration on both weekdays and weekends starts to slightly decline (Figure 10). The 4th highest concentrations in each year that are similar to $O_3$ design value are also calculated for weekdays and weekends separately for the 16 sites in Figure 10. This plot shows that the 4th highest values are larger on weekdays than on weekends in the 1980s and are similar on weekdays and weekends in the 1990s. In the 2000s, the 4th highest values are larger on weekends than on weekdays. In the 2010s, the 4th highest values on weekdays and weekends are getting almost identical from 2010 to the mid of 2010 and the weekday values are getting larger than the weekends values from the mid of 2010 and onward. The observed and simulated $O_3$ concentrations in this study indicate dynamic changes in emissions and photochemistry leading to the status of the identical weekday and weekend $O_3$ concentrations, turning from "VOC-limited"

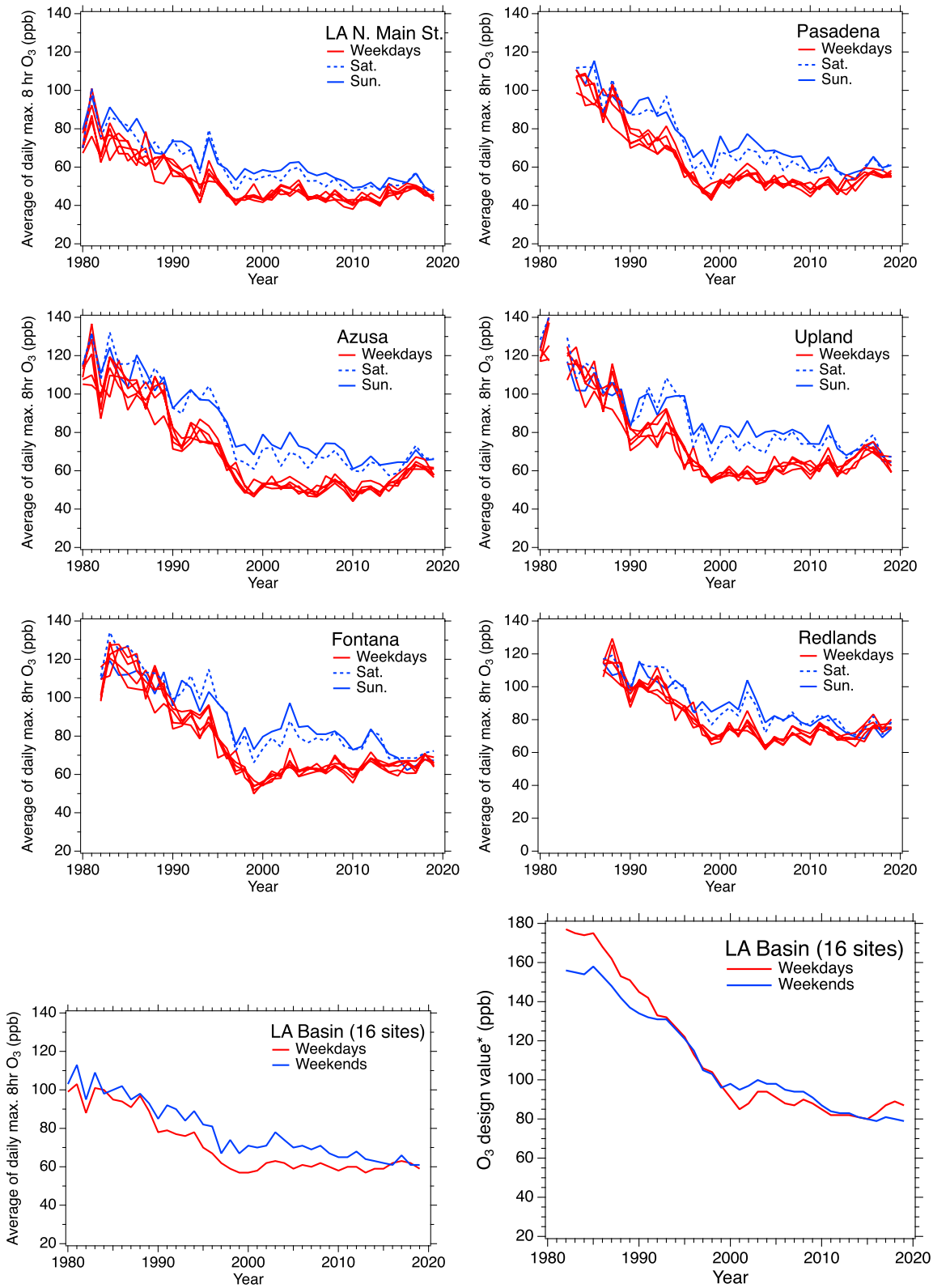


**Figure 10.** Trends in averages of daily maximum 8hr-average observed $O_3$ during weekdays and weekends at several monitoring sites in the Los Angeles Basin from 1980 to 2019. The averages for 16 sites in the Los Angeles Basin are also shown (bottom). The red lines (blue lines) represent weekdays (weekends). The data covering May-September are utilized. *$O_3$ design values here are calculated separately for weekdays and weekends. The 16 sites correspond to the sites in Figure 1.

to "$NO_x$-limited" regimes for the first time in several decades, which hints at the success of the environmental policies made for $O_3$ compliance.

## 4. Conclusions

For multiple decades, extensive efforts have been made to reduce tropospheric $O_3$ and its precursor concentrations in the LA Basin. However, even though significant strides have been made in reducing $O_3$ levels compared to the 1960s, there is still a need for improvement to meet the National Ambient Air Quality Standards. In this study, using air quality monitoring observations and air quality model simulations, we assessed the effectiveness of long-term pollution regulations on $O_3$ concentrations in the Los Angeles region. In particular, we highlighted the changes from the past one or two decades in which the average $O_3$ concentrations did not show clear improvements despite large decreases in precursor concentrations. Our chemical modeling involves major emission changes in the past decades as well as expected changes in the future. Both the surface monitor observations and our model results revealed substantial changes in the photochemical regime in the Basin. This was manifested by changes in the differences between $O_3$ concentrations on weekdays and weekends. The take-away point of this study is that the weekend $O_3$ effect (higher $O_3$ concentrations on weekends than on weekdays caused by non-linear photochemistry) is not observed and simulated any more in the late 2010s: $O_3$ concentrations averaged for weekdays and weekends are almost the same and show a sign of decreasing together with time. Note that $NO_2$ concentrations also decrease with time persistently during this time period. Thus, it confirms that the photochemical regime turns from "VOC-limited" to "$NO_x$-limited" regime in the late 2010s and 2020s, according to the model predictions. This study indicates that the pollution control policies and practices has had a measurable effect on reducing $O_3$ pollution. Our study indicates that further reductions of $NO_x$ emissions from the present could contribute to further decreases of $O_3$ concentrations in the LA Basin.

The scenario model runs were based on the same meteorology in 2010 to emphasize the effects of anthropogenic emission changes on surface $O_3$ abundances. The increases of air temperature under the influence of climate change can aggravate $O_3$ pollution (e.g., Jacob & Winner, 2009; Nussbaumer & Cohen, 2021). Future research would need to consider various meteorological scenarios as well as emission scenarios to design $O_3$ reduction paths including climate penalties. It would also be essential to address the impact of wildfires and global/Asian emissions on $O_3$ in the LA Basin and its surrounding area.

## Data Availability Statement

The WRF-Chem model version 3.4.1 used in this study is available at http://www2.mmm.ucar.edu/wrf/users/download/get_source.html. The long-term surface observations of $NO_2$, CO, and $O_3$ were downloaded from https://aqs.epa.gov/aqsweb/airdata/download_files.html.

**Acknowledgments**
The NOAA Health of Atmosphere program and the NASA ROSES ACMAP (NNH14AX01I) supported this research. This subject is also supported by the National Research Foundation of Korea (NRF) grant funded by the Korea government (MSIT; No. 2020R1A2C2014131). S.-W. Kim also acknowledges support from NRF-2018R1A5A1024958.

## References

Ahmadov, R., McKeen, S., Trainer, M., Banta, R., Brewer, A., Brown, S., et al. (2015). Understanding high wintertime ozone pollution events in an oil- and natural gas-producing region of the western US. *Atmospheric Chemistry and Physics*, *15*, 411–429. https://doi.org/10.5194/acp-15-411-2015

Baidar, S., Hardesty, R. M., Kim, S.-W., Langford, A. O., Oetjen, H., Senff, C., et al. (2015). Weakening of the weekend ozone effect over California's South Coast Air Basin. *Geophysical Research Letters*, *42*, 9457–9464. https://doi.org/10.1002/2015GL066419

Ban-Weiss, G. A., McLaughlin, J. P., Harley, R. A., Lunden, M. M., Kirchstetter, T. W., Kean, A. J., et al. (2008). Long-term changes in emissions of nitrogen oxides and particulate matter from on-road gasoline and diesel vehicles. *Atmospheric Environment*, *42*(2), 220–232. https://doi.org/10.1016/j.atmosenv.2007.09.049

Bauwens, M., Compernolle, S., Stavrakou, T., Müller, J.-F., van Gent, J., Eskes, H., et al. (2020). Impact of Coronavirus outbreak on $NO_2$ pollution assessed using TROPOMI and OMI observations. *Geophys. Res. Lett.*, *47*, e2020GL. https://doi.org/10.1029/2020gl087978

Berrisford, P., Dee, D. P., Poli, P., Brugge, R., Fielding, K., Fuentes, M., et al. (2011). *The ERA-interim archive version 2.0. ERA report series 1*. Retrieved from http://www.ecmwf.int/en/elibrary/8174-era-interim-archive-version-20

Bishop, G. A., & Stedman, D. H. (2008). A decade of on-road emissions measurements. *Environmental Science & Technology*, *42*(5), 1651–1656. https://doi.org/10.1021/es702413b

Boersma, K. F., Eskes, H. J., Dirksen, R. J., van der A, R. J., Veefkind, J. P., Stammes, P., et al. (2011). An improved tropospheric $NO_2$ column retrieval algorithm for the Ozone Monitoring Instrument. *Atmospheric Measurement Techniques*, *4*, 1905–1928. https://doi.org/10.5194/amt-4-1905-2011

California Air Resources Board. (2009). *CEPAM: 2009 almanac-standard emissions tool*. CARB.

California Air Resources Board. (2015). *California motor vehicle emission factor/emission inventory model (EMFAC 2014)*. CARB.

California Air Resources Board. (2016). *CEPAM: 2016 SIP almanac - standard emissions tool*. CARB.

Chen, D., Li, Q., Stutz, J., Mao, Y., Zhang, L., Pikelnaya, O., et al. (2013). WRF-Chem simulation of $NO_x$ and $O_3$ in the L.A. basin during CalNex-2010. *Atmospheric Environment*, *81*, 421–432. https://doi.org/10.1016/j.atmosenv.2013.08.064

Coggon, M. M., Gkatzelis, G. I., McDonald, B. C., Gilman, J. B., Schwantes, R. H., Aikin, K. C., et al. (2021). Volatile chemical product emissions enhance ozone and modulate urban chemistry. *Proceedings of the National Academy of Sciences of the United States of America*, *118*(32). https://doi.org/10.1073/pnas.2026653118

Demetillo, M. A. G., Anderson, J. F., Geddes, J. A., Yang, X., Najacht, E. Y., Herrera, S. A., et al. (2019). Observing severe drought influences on ozone air pollution in California. *Environmental Science & Technology*, *53*, 4695–4706. https://doi.org/10.1021/acs.est.8b04852

Dixit, P., Miller, J. W., Cocker, D. R., Oshinuga, A., Jiang, Y., Durbin, T. D., & Johnson, K. C. (2017). Differences between emissions measured in urban driving and certification testing of heavy-duty diesel engines. *Atmospheric Environment*, *166*, 276–285. https://doi.org/10.1016/j.atmosenv.2017.06.037

Dunlea, E. J., Herndon, S. C., Nelson, D. D., Volkamer, R. M., San Martini, F., Sheehy, P. M., et al. (2007). Evaluation of nitrogen dioxide chemiluminescence monitors in a polluted urban environment. *Atmospheric Chemistry and Physics*, *7*, 2691–2704. https://doi.org/10.5194/acp-7-2691-2007

EPA. (1995). *Study of volatile organic compound emissions from consumer and commercial products*. EPA-453/R-94-066-A. EPA.

Fehsenfeld, F. C., Dickerson, R. R., Hübler, G., Luke, W. T., Nunnermacker, L. J., Williams, E. J., et al. (1987). A ground-based intercomparison of NO, $NO_x$, and $NO_y$ measurement techniques. *Journal of Geophysical Research: Atmospheres*, *92*(D12), 14710–14722. https://doi.org/10.1029/jd092id12p14710

Fujita, E. R., Stockwell, W. R., Campbell, D. E., Keislar, R. E., & Lawson, D. R. (2003). Evolution of the magnitude and spatial extent of the weekend ozone effect in California's South Coast Air Basin, 1981–2000. *Journal of the Air & Waste Management Association*, *53*(7), 802–815. https://doi.org/10.1080/10473289.2003.10466225

Gkatzelis, G. I., Coggon, M. M., McDonald, B. C., Peischl, J., Gilman, J. B., Aikin, K. C., et al. (2021). Observations confirm that volatile chemical products are a major source of petrochemical emissions in U.S. cities. *Environmental Science & Technology*, *55*(8), 4332–4343. https://doi.org/10.1021/acs.est.0c05471

Grell, G. A., Peckham, S. E., Schmitz, R., McKeen, S. A., Frost, G., Skamarock, W. C., & Eder, B. (2005). Fully coupled "online" chemistry within the WRF model. *Atmospheric Environment*, *39*(37), 6957–6975. https://doi.org/10.1016/j.atmosenv.2005.04.027

Guenther, A., Karl, T., Harley, P., Wiedinmyer, C., Palmer, P. I., & Geron, C. (2006). Estimates of global terrestrial isoprene emissions using MEGAN (model of emissions of Gases and aerosols from nature). *Atmospheric Chemistry and Physics*, *6*, 3181–3210. https://doi.org/10.5194/acp-6-3181-2006

Haagen-Smit, A. J. (1952). Chemistry and physiology of Los Angeles smog. *Industrial & Engineering Chemistry*, *44*(6), 1342–1346. https://doi.org/10.1021/ie50510a045

Harkins, C., McDonald, B. C., Henze, D. K., & Wiedinmyer, C. (2021). A fuel-based method for updating mobile source emissions during the COVID-19 pandemic. *Environmental Research Letters*, *16*, 065018. https://doi.org/10.1088/1748-9326/ac0660

Harley, R. A., Hannigan, M. P., & Cass, G. R. (1992). Respeciation of organic gas emissions and the detection of excess unburned gasoline in the atmosphere. *Environmental Science & Technology*, *26*(12), 2395–2408. https://doi.org/10.1021/es00036a010

Harley, R. A., Marr, L. C., Lehner, J. K., & Giddings, S. N. (2005). Changes in motor vehicle emissions on diurnal to decadal time scales and effects on atmospheric composition. *Environmental Science & Technology*, *39*(14), 5356–5362. https://doi.org/10.1021/es048172+

Harley, R. A., Russell, A. G., & Cass, G. R. (1993b). Mathematical modeling of the concentrations of volatile organic compounds: Model performance using a lumped chemical mechanism. *Environmental Science & Technology*, *27*, 1638–1649. https://doi.org/10.1021/es00045a022

Harley, R. A., Russell, A. G., McRae, G. J., Cass, G. R., & Seinfeld, J. H. (1993a). Photochemical modeling of the southern California air quality study. *Environmental Science & Technology*, *27*, 378–388. https://doi.org/10.1021/es00039a019

Harley, R. A., Sawyer, R. F., & Milford, J. B. (1997). Updated photochemical modeling for California's South Coast Air Basin: Comparison of chemical mechanisms and motor vehicle emission inventories. *Environmental Science & Technology*, *31*, 2829–2839. https://doi.org/10.1021/es9700562

Hassler, B., McDonald, B. C., Frost, G. J., Borbon, A., Carslaw, D. C., Civerolo, K., et al. (2016). Analysis of long-term observations of NOx and CO in megacities and application to constraining emissions inventories. *Geophysical Research Letters*, *43*(18), 9920–9930. https://doi.org/10.1002/2016gl069894

Jacob, D. J., & Winner, D. A. (2009). Effect of climate change on air quality. *Atmospheric Environment*, *43*(1), 51–63. https://doi.org/10.1016/j.atmosenv.2008.09.051

Jacobson, M. Z. (2005). *Fundamentals of atmospheric modeling* (2nd ed.). Cambridge University Press. https://doi.org/10.1017/CBO9781139165389

Jacobson, M. Z., Lu, R., Turco, R. P., & Toon, O. B. (1996). Development and application of a new air pollution model system-part I: Gas-phase simulations. *Atmospheric Environment*, *30*(12), 1939–1963. https://doi.org/10.1016/1352-2310(95)00139-5

Jaffe, D. A., Cooper, O. R., Fiore, A. M., Henderson, B. H., Tonnesen, G. S., Russell, A. G., et al. (2018). Scientific assessment of background ozone over the U.S.: Implications for air quality management. *Elementa: Science of the Anthropocene*, *6*, 56. https://doi.org/10.1525/elementa.309

Kim, S.-W., Heckel, A., Frost, G. J., Richter, A., Gleason, J., Burrows, J. P., et al. (2009). $NO_2$ columns in the western United States observed from space and simulated by a regional chemistry model and their implications for $NO_x$ emissions. *Journal of Geophysical Research: Atmospheres*, *114*(D11), D11301. https://doi.org/10.1029/2008JD011343

Kim, S.-W., McDonald, B. C., Baidar, S., Brown, S. S., Dube, B., Ferrare, R. A., et al. (2016). Modeling the weekly cycle of $NO_x$ and CO emissions and their impacts on $O_3$ in the LosAngeles-South Coast Air Basin during the CalNex 2010 field campaign. *Journal of Geophysical Research: Atmospheres*, *121*(3), 1340–1360. https://doi.org/10.1002/2015JD024292

Kim, S.-W., McKeen, S. A., Frost, G. J., Lee, S.-H., Trainer, M., Richter, A., et al. (2011). Evaluations of $NO_x$ and highly reactive VOC emission inventories in Texas and their implications for ozone plume simulations during the Texas Air Quality Study 2006. *Atmospheric Chemistry and Physics*, *11*(22), 11361–11386. https://doi.org/10.5194/acp-11-11361-2011

Lamsal, L. N., Krotkov, N. A., Vasilkov, A., Marchenko, S., Qin, W., Yang, E.-S., et al. (2021). Ozone Monitoring Instrument (OMI) Aura nitrogen dioxide standard product version 4.0 with improved surface and cloud treatments. *Atmospheric Measurement Techniques*, *14*(1), 455–479. https://doi.org/10.5194/amt-14-455-2021

Lawson, D. R. (1990). The southern California air-quality study. *Journal of the Air & Waste Management Association*, *40*(2), 156–165. https://doi.org/10.1080/10473289.1990.10466671

Levelt, P. F., Joiner, J., Tamminen, J., Veefkind, J. P., Bhartia, P. K., Stein Zweers, D. C., et al. (2018). The ozone monitoring instrument: Overview of 14 years in space. *Atmospheric Chemistry and Physics*, *18*, 5699–5745. https://doi.org/10.5194/acp-18-5699-2018

Levelt, P. F., van den Oord, G. H. J., Dobber, M. R., Mälkki, A., Visser, H., de Vries, J., et al. (2006). The ozone monitoring instrument. *IEEE Transactions on Geoscience and Remote Sensing*, *44*(5), 1093–1101. https://doi.org/10.1109/TGRS.2006.872333

Lin, M., Horowitz, L. W., Xie, Y., Paulot, F., Malyshev, S., Shevliakova, E., et al. (2020). Vegetation feedbacks during drought exacerbate ozone air pollution extremes in Europe. *Nature Climate Change*, *10*, 444–451. https://doi.org/10.1038/s41558-020-0743-y

Lin, M., Horowitz, L. W., Payton, R., Fiore, A. M., & Tonnesen, G. (2017). US surface ozone trends and extremes from 1980 to 2014: quantifying the roles of rising Asian emissions, domestic controls, wildfires, and climate. *Atmospheric Chemistry and Physics*, *17*(4), 2943–2970. https://doi.org/10.5194/acp-17-2943-2017

Lu, R., Turco, R. P., & Jacobson, M. Z. (1997). An integrated air pollution modeling system for urban and regional scales: 2. Simulations for SCAQS 1987. *Journal of Geophysical Research: Atmospheres*, *102*(D5), 6081–6098. https://doi.org/10.1029/96jd03502

Marr, L. C., & Harley, R. A. (2002). Modeling the effect of weekday-weekend differences in motor vehicle emissions on photochemical air pollution in central California. *Environmental Science & Technology*, *36*, 4099–4106. https://doi.org/10.1021/es020629x

Martien, P. T., & Harley, R. A. (2006). Adjoint sensitivity analysis for a three-dimensional photochemical model: Application to southern California. *Environmental Science & Technology*, *40*, 4200–4210. https://doi.org/10.1021/es051026z

McDonald, B. C., Dallmann, T. R., Martin, E. W., & Harley, R. A. (2012). Long-term trends in nitrogen oxide emissions from motor vehicles at national, state, and air basin scales. *Journal of Geophysical Research: Atmospheres*, *117*(D21), D00V18. https://doi.org/10.1029/2012JD018304

McDonald, B. C., de Gouw, J. A., Gilman, J. B., Jathar, S. H., Akherati, A., Cappa, C. D., et al. (2018). Volatile chemical products emerging as largest petrochemical source of urban organic emissions. *Science*, *359*(6377), 760–764. https://doi.org/10.1126/science.aaq0524

McDonald, B. C., Gentner, D. R., Goldstein, A. H., & Harley, R. A. (2013). Long-term trends in motor vehicle emissions in U.S. urban areas. *Environmental Science & Technology*, *46*, 10022–10031. https://doi.org/10.1021/es401034z

McDonald, B. C., Goldstein, A. H., & Harley, R. A. (2015). Long-term trends in California mobile source emissions and ambient concentrations of black carbon and organic aerosol. *Environmental Science & Technology*, *49*(8), 5178–5188. https://doi.org/10.1021/es505912b

McDonald, B. C., McBride, Z. C., Martin, E. W., & Harley, R. A. (2014). High-resolution mapping of motor vehicle carbon dioxide emissions. *Journal of Geophysical Research: Atmospheres*, *119*, 5283–5298. https://doi.org/10.1002/2013JD021219

McDonald, B. C., McKeen, S. A., Cui, Y. Y., Ahmadov, R., Kim, S.-W., Frost, G. J., et al. (2018). Modeling ozone in the Eastern U.S. Using a fuel-based mobile source emissions inventory. *Environmental Science & Technology*, *52*(13), 7360–7370. https://doi.org/10.1021/acs.est.8b00778

National Research Council. (1991). *Rethinking the ozone problem in urban and regional air pollution*. National Academic Press.

Nussbaumer, C. M., & Cohen, R. C. (2021). Impact of OA on the temperature dependence of PM2.5 in the Los Angeles basin. *Environmental Science & Technology*, *55*(6), 3549–3558. https://doi.org/10.1021/acs.est.0c07144

Parrish, D. D., Kuster, W. C., Shao, M., Yokouchi, Y., Kondo, Y., Goldan, P. D., et al. (2009). Comparison of air pollutant emissions among mega-cities. *Atmospheric Environment*, *43*(40), 6435–6441. https://doi.org/10.1016/j.atmosenv.2009.06.024

Pollack, I. B., Ryerson, T. B., Trainer, M., Neuman, J. A., Roberts, J. M., & Parrish, D. D. (2013). Trends in ozone, its precursors, and related secondary oxidation products in Los Angeles, California: A synthesis of measurements from 1960 to 2010. *Journal of Geophysical Research: Atmospheres*, *118*, 5893–5911. https://doi.org/10.1002/jgrd.50472

Pollack, I. B., Ryerson, T. B., Trainer, M., Parrish, D. D., Andrews, A. E., Atlas, E. L., et al. (2012). Airborne and ground-based observations of a weekend effect in ozone, precursors, and oxidation products in the California South Coast Air Bain. *Journal of Geophysical Research: Atmospheres*, *117*(D21), D00V05. https://doi.org/10.1029/2011JD016772

Qin, M., Murphy, B. N., Isaacs, K. K., McDonald, B. C., Lu, Q., McKeen, S. A., et al. (2021). Criteria pollutant impacts of volatile chemical products informed by near-field modeling. *Nature Sustainability*, *4*, 129–137. https://doi.org/10.1038/s41893-020-00614-1

Russell, A. R., Valin, L. C., & Cohen, R. C. (2012). Trends in OMI $NO_2$ observations over the United States: effects of emission control technology and the economic recession. *Atmospheric Chemistry and Physics*, *12*(24), 12197–12209. https://doi.org/10.5194/acp-12-12197-2012

Ryerson, T. B., Andrews, A. E., Angevine, W. M., Bates, T. S., Brock, C. A., Cairns, B., et al. (2013). The 2010 California research at the Nexus of air quality and climate change (CalNex) field study. *Journal of Geophysical Research: Atmospheres*, *118*(11), 5830–5866. https://doi.org/10.1002/jgrd.50331

Shah, R. U., Coggon, M. M., Gkatzelis, G. I., McDonald, B. C., Tasoglou, A., Huber, H., et al. (2020). Urban oxidation Flow reactor measurements reveal significant secondary organic aerosol contributions from volatile emissions of emerging importance. *Environmental Science & Technology*, *54*(2), 714–725. https://doi.org/10.1021/acs.est.9b06531

Simon, H., Reff, A., Wells, B., Xing, J., & Frank, N. (2015). Ozone trends across the United States over a period of decreasing $NO_x$ and VOC emissions. *Environmental Science & Technology*, *49*, 186–195. https://doi.org/10.1021/es504514z

Stockwell, C. E., Coggon, M. M., Gkatzelis, G. I., Ortega, J., McDonald, B. C., Peischl, J., et al. (2021). Volatile organic compound emissions from solvent- and water-borne coatings-compositional differences and tracer compound identifications. *Atmospheric Chemistry and Physics*, *21*(8), 6005–6022. https://doi.org/10.5194/acp-21-6005-2021

Stockwell, W. R., Kirchner, F., Kuhn, M., & Seefeld, S. (1997). A new mechanism for regional atmospheric chemistry modeling. *Journal of Geophysical Research: Atmospheres*, *102*(D22), 25847–25879. https://doi.org/10.1029/97jd00849

Tan, Y., Henderick, P., Yoon, S., Herner, J., Montes, T., Boriboonsomsin, K., et al. (2019). On-board sensor-based $NO_x$ emissions from heavy-duty diesel vehicles. *Environmental Science & Technology*, *53*(9), 5504–5511. https://doi.org/10.1021/acs.est.8b07048

U.S. Bureau of Transportation Statistics. (1996). *1993 commodity flow survey*. US Department of Transportation.

U.S. Census Bureau. (1995). *Economic census survey, census of manufactures*. US Department of Commerce.

Warneke, C., de Gouw, J. A., Edwards, P. M., Holloway, J. S., Gilman, J. B., Kuster, W. C., et al. (2013). Photochemical aging of volatile organic compounds in the Los Angeles basin: Weekday-weekend effect. *Journal of Geophysical Research: Atmospheres*, *118*(10), 5018–5028. https://doi.org/10.1002/jgrd.50423

Warneke, C., de Gouw, J. A., Holloway, J. S., Peischl, J., Ryerson, T. B., Atlas, E., et al. (2012). Multiyear trends in volatile organic compounds in Los Angeles, California: Five decades of decreasing emissions. *Journal of Geophysical Research: Atmospheres*, *117*(D21), D00V17. https://doi.org/10.1029/2012JD017899

Yan, Y., Lin, J., & He, C. (2018). Ozone trends over the United States at different times of day. *Atmospheric Chemistry and Physics*, *18*, 1185–1202. https://doi.org/10.5194/acp-18-1185-2018

Yu, K., McDonald, B. C., & Harley, R. A. (2021). Evaluation of nitrogen oxide emission inventories and trends for on-road gasoline and diesel vehicles. *Environmental Science & Technology*, *55*, 6655–6664. https://doi.org/10.1021/acs.est.1c00586

Zhu, S., Kinnon, M. M., Shaffer, B. P., Samuelsen, G. S., Brouwer, J., & Dabdub, D. (2019). An uncertainty for clean air: Air quality modeling implications of underestimating VOC emissions in urban inventories. *Atmospheric Environment*, *211*, 256–267. https://doi.org/10.1016/j.atmosenv.2019.05.019